The use of MSE walls backfilled with Lightweight Cellular Concrete in soft ground seismic areas

El uso de muros MSE rellenados con hormigón celular ligero en áreas sísmicas donde los terrenos son blandos

Daniel Pradel [1&2] and Binod Tiwari[3]

[1]Adjunct Associate Professor, University of California Los Angeles (UCLA), Los Angeles, California (dpradel@ucla.edu) &
[2]Vice-President, Shannon & Wilson, 664 W. Broadway, Glendale, California (dep@shanwil.com)
[3]Professor, California State University Fullerton (CSUF), Fullerton California (btiwari@csuf.edu)

ABSTRACT: A series of numerical analyses were performed on a Mechanically Stabilized Earth (MSE) wall that used Lightweight Cellular Concrete (LCC) instead of soil as infill. These analyses were performed using the geometry and input ground motions for a wall recently built for the Silicon Valley Rapid Transit (SVRT) system near San Francisco, California. For our analyses, the LCC-MSE wall was significantly weakened in our numerical models by using shortened geogrid lengths, and lower material strengths than the constructed wall. In spite of the weakened nature of the wall analyzed herein, seismic failure of the LCC materials and supporting ground was not predicted. Our analyses show that well designed LCC-MSE walls tend to move dynamically in a quasi-rigid fashion, i.e., that they move mainly laterally and do not exhibit major rocking or seismic settlements. Additionally, because of their broad base of MSE walls, these walls distribute compressive and shear stresses to the underlying ground in a relatively even manner. Our numerical analyses also show that internal reinforcement of LCC-MSE walls is important to restrain side panels during earthquakes, but that the inertial loads from the panels are quickly transferred to the LCC. Hence, that long or continuous reinforcements are not needed for seismic stability. In summary, our analyses show that LCC is an excellent material for MSE walls and that the lightening of vertical loads that LCC provides has distinct seismic advantages in soft ground seismic areas, e.g., the elimination of ground improvement.

RESUMEN: Análisis numéricos fueron completados para un muro de tipo MSE que fue rellenado con hormigón celular ligero en vez de tierra. Los análisis que presentados aquí fueron conducidos usando la geometría y sismicidad de un muro recientemente construido para trenes de la red SVRT cerca de San Francisco, California. Una diferencia notable entre el muro construido y el muro analizado, es que usamos resistencias más bajas y menos refuerzos en nuestros cálculos. A pesar de eso, nuestros cálculos no lograron predecir la ruptura de materiales. Nuestros análisis muestran que este tipo de muro se comporta de manera casi rígida, con movimientos primordialmente horizontales, y poca rotación o asentamientos dinámicos. Como este tipo de muro tiene una base ancha los esfuerzos verticales tienden a repartirse de manera relativamente uniforme en los suelos bajo el muro. Nuestros análisis también muestran que los refuerzos de tipo geogrid son importantes para aguantar dinámicamente a los paneles laterales, pero que los esfuerzos de tensión en los refuerzos son rápidamente transmitidos al hormigón celular ligero. Por lo tanto refuerzos largos o continuos no son necesarios para la estabilidad dinámica. En resumen, nuestros análisis muestran que el hormigón celular ligero es un excelente material para muros de tipo MSE y que el aligeramiento que proporciona el hormigón celular ligero tiene importantes ventajas sísmicas en zonas con tierras blandas, como el eliminar el amejoramiento de los suelos de fundación.

1 INTRODUCTION

Soft-ground construction poses significant geotechnical challenges, ranging from large consolidation settlements (below the structure and in nearby developments), construction staging and extended project schedules. In seismic regions, soft ground conditions often result in the significant amplification of structural demands. For freeway and railroad embankments, such demands often result in costly ground improvement to mitigate the significant consolidation settlements resulting from the heavy weight of Mechanically Stabilized Earth (MSE) walls.

Recently, a novel approach for the construction of MSE walls has been used, which involves replacing the MSE's soil infill with Lightweight Cellular Concrete (LCC). The main advantage of LCC is its low unit weight (often about half the unit weight of water). In California, examples of LCC-MSE walls include the Colton Crossing for the Union Pacific-BNSF railroad in Colton (Teig and Anderson, 2012), the San Bruno Railroad Grade Separation in San Bruno, and the

Silicon Valley Berryessa Extension in San Jose which will connect the Silicon Valley Rapid Transit (SVRT) system to San Francisco's Bay Area Rapid Transit (BART) system.

In addition to railroad projects, LCC-MSE walls have also been used and/or are being considered for road transportation projects such as the 22/405 freeway interchange in Orange County, California, as well as for various new bridge approaches.

Figure 1. Lightweight Cellular Concrete.

Figure 2. Construction of an LCC- MSE wall (Cell-Crete, 2015).

One of the main advantages of LCC is a reduction of up to 75% in the static weight of a traditional MSE walls. This significant weight reduction, results in much lower consolidation settlements, as well as reduced inertial loads and dynamic compression during earthquakes.

The excavation of relatively heavy on-site soils for the wall foundations, combined with the low unit weight of LCC (compared to soil) can result in a balanced design (with zero added bearing pressures) or a small net increase in the foundation soils' vertical stresses. This has allowed designers to either completely eliminate the need for improving the soft subgrade (e.g., eliminating stone columns) under certain MSE walls or at least to significantly reduce the scope of ground improvement (e.g., limited vibro-replacement in Teig and Anderson, 2012).

An advantage of using LCC as fill, is that the relatively high strength of this material (compared to conventional MSE granular fill) also results in essentially no lateral "earth" pressures on the MSE panels and abutment walls.

The weight advantages of LCC are shared by other materials, such as Geofoam. However, Geofoam is combustible and reacts chemically with hydrocarbons such as diesel fuel. Hence, railroads have been reluctant to accept Geofoam structures in California, but have often accepted the use of LCC.

2 CONSTRUCTION OF LCC-MSE WALLS

2.1 *Nature and Physical Properties of LCC*

Lightweight Cellular Concrete (ACI, 2006) is created by adding stable air cells during the manufacture of the material (Figure 1), and LCC is placed in a manner quite similar to concrete (Figure 2). Relatively few MSE walls with LCC as infill have been built in seismic areas and its use is generally considered a novel practice.

The manufactured process of LCC results in a concrete preformed foam that has very low densities, low thermal conductivities, and high strengths compared to that of a conventional MSE soil infill. Its nature and behavior is often described as similar to that of porous soft rock.

In California, the design engineer generally specifies a minimum compressive strength for the LCC material that the supplier (or manufacturer) must deliver during construction. It is not unusual to have two or more minimum strengths specified by the design engineer for the same wall, e.g., a higher strength near the foundation soils and lower strengths in the upper portions of the wall. In our experience, densities of LCC used for MSE walls in California typically range from about 300 kg/m^3 to about 600 kg/m^3. The strength of LCC correlates strongly with the density of the material; for the above range of densities, the average uniaxial compressive strengths of LCC materials, of the type used in MSE walls in California are typically between 500 and 3,000 kPa.

2.2 *Construction of LCC-MSE walls*

Except for the foundations, the LCC in MSE walls is generally formed between the facing panels (Figures 2 to 5). These panels play an important protective role as LCC is not as strong as conventional concrete and can be relatively easily damaged, e.g., by a small vehicle impact. The facing panels are anchored to the wall through reinforcements, as in conventional MSE walls.

In our experience, LCC-MSE walls have typically been reinforced with metal straps, steel rods and geogrids (Figures 3 to 5). The reinforcement of the

LCC in MSE walls is sometimes continuous (as in Figure 3), or limited in length to the area near the outer face (as shown in Figure 4).

Figure 3. Placement of LCC over continuous geogrid reinforcement, within the panels of an MSE wall being built for the SVRT system near San Jose, California (design of wall detailed in GDC, 2014).

Figure 4. LCC placement in an MSE wall reinforced with metal straps near the facing panels (Cell-Crete, 2015).

Figure 5. LCC placement by in an MSE wall reinforced with steel rods (Cell-Crete, 2015).

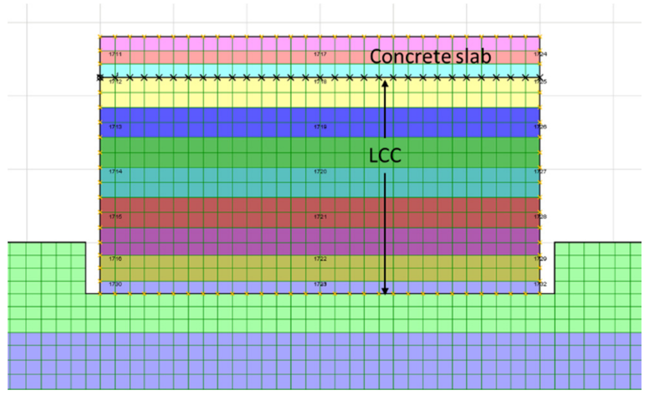

Figure 6. FLAC model including geometry of LCC and subsurface soft soil profile (each underlying grid is 3.3 m = 10 feet).

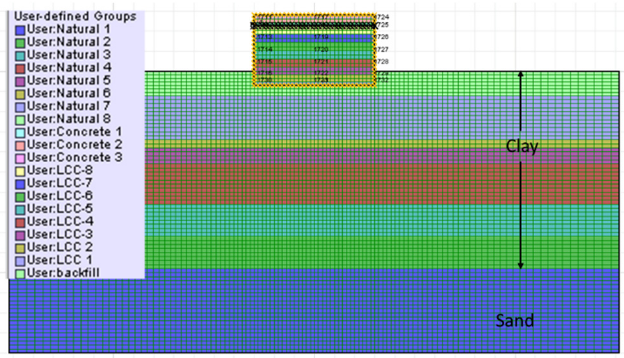

Figure 7. Detail of FLAC model including geometry of LCC and concrete slab. Stage shown is before backfilling next to wall (each underlying grid is 3.3 m = 10 feet)

3 NUMERICAL MODELING

3.1 *Introduction*

To understand the seismic behavior of a geogrid reinforced LCC-MSE wall we conducted numerical analyses using the computer program FLAC version 7.0 from Itasca (2011). For the analyses shown herein, we adopted the subsurface conditions, wall geometry and seismic design loads of an LCC-MSE wall that was recently completed in 2014-2015 for the Silicon Valley Rapid Transit (SVRT) in San Jose, California (shown in Figure 3). This project will extend subway service from San Francisco to San Jose.

The adopted model geometry for the LCC-MSE wall is shown in Figures 6 and 7. It includes about 9 m of LCC materials built in 8 stages (about 2 m below and 7 m above final grade), and a rolling slab about 1.5 m thick at the top composed of conventional reinforced concrete.

Since, in our opinion, the SVRT wall (being built in Figure 3) was well designed but very conservative, we decided to analyze a weakened version of the constructed wall. As a result, certain aspects of our numerical analyses are significantly different than those used for the original design by the design engineers as well as the final construction. For example: (a) the geotechnical consultant's numerical analyses did not include geogrid elements in their FLAC models (GDC, 2014), (b) the final construction incorporated full length geogrid between the panels (as shown in Figure 3), (c) in our analyses geogrid reinforcement only extends 1/3 of the length between the walls, (d) we used reduced (lower values) LCC strengths than specified during construction, and (e) we used in FLAC the dynamic properties obtained from cyclic simple shear tests recently performed at California State University Fullerton (Tiwari, 2015a & 2015b) for the Cell-Crete corporation (Cell-Crete, 2015). Please note that Professor Tiwari's triaxial and dynamic simple shear tests were performed on a large number of LCC samples that were prepared for different sets of LCC densities, and that we used only the data that was the most appropriate for the adopted LCC density in our analyses, i.e., 480 kg/m^3.

In summary, the analyses presented herein, should be considered applicable to a hypothetical MSE wall that has a geometry similar to the one shown in Figure 3, but that is purposely much weaker. The differences between the constructed and analyzed wall are considered substantial.

3.2 *Adopted Properties of concrete and LCC Materials*

Both the heavy reinforced concrete slab and LCC materials were modeled as elastoplastic materials with a compressive strength of 20,000 kPa and 275 kPa, respectively. Please note that the adopted LCC strength is conservative for the specified density of 480 kg/m^3. As previously indicated, our adopted LCC compressive strengths are significantly lower than the strength specified for the constructed wall in Figure 3, where we understand minimum LCC strengths around 550 kPa were ultimately required and vastly exceeded by the LCC supplier (Cell-Crete).

3.3 *Dynamic Properties of soils and LCC Materials*

The shear wave velocities near subject site and in San Jose, California, are known to considerable depths and have been the subject of numerous studies. Typical shear wave velocity profiles are reported in Chiu et al. (2008) for depths of 0 to 410 m (including the deep suspension logging performed by the USGS).

For our numerical analyses, we used both the specific shear wave velocities obtained from the site's subsurface characterization (GDC, 2014) as well as the deeper data in Chiu et al. (2008). The adopted shear wave velocities varied linearly in clays from 150 m/s at the surface to 300 m/s a depth of 30 m. Sand layers below 30 m were modeled with a constant 450 m/s velocity. Similarly, undrained shear strength varied from about 75 kPa near the surface to about 160 kPa at a depth of 30 m.

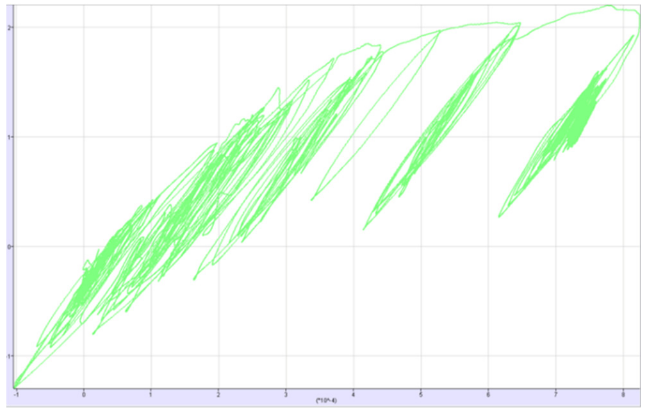

Figure 8. Accumulation of permanent shear strains and hysteretic damping in FLAC based on Massing (1926) rule.

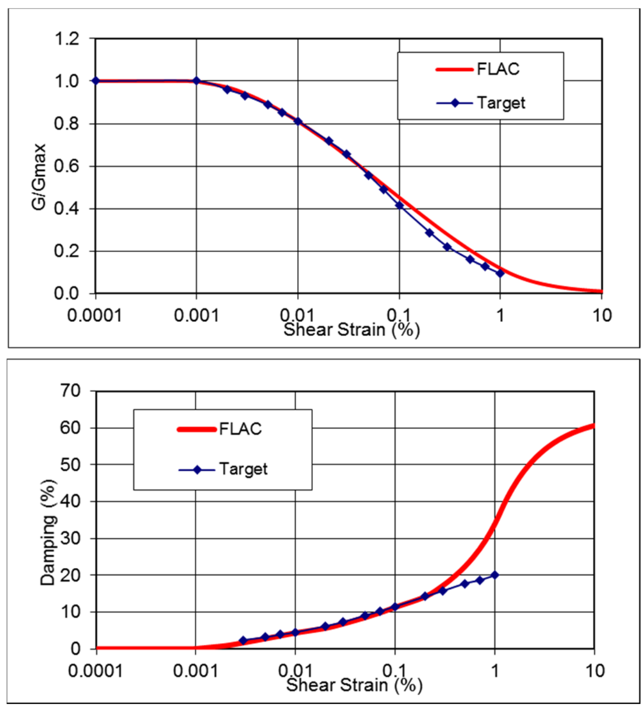

Figure 9. Matching of modulus reduction and damping curves used for clays and Vucetic & Dobry experiments (1991).

To allow damping to vary with time during dynamic loading in FLAC, we adopted, for simplicity, hysteretic damping based on the Massing (1926) rule and we used as backbone the shear moduli curves at specific depths. This technique allows the accumulation of shear strains during dynamic loading as shown in Figure 8. Please note that a small amount of Rayleigh damping of 0.2% was added for numerical stability as well as energy dissipation at small loading cycles.

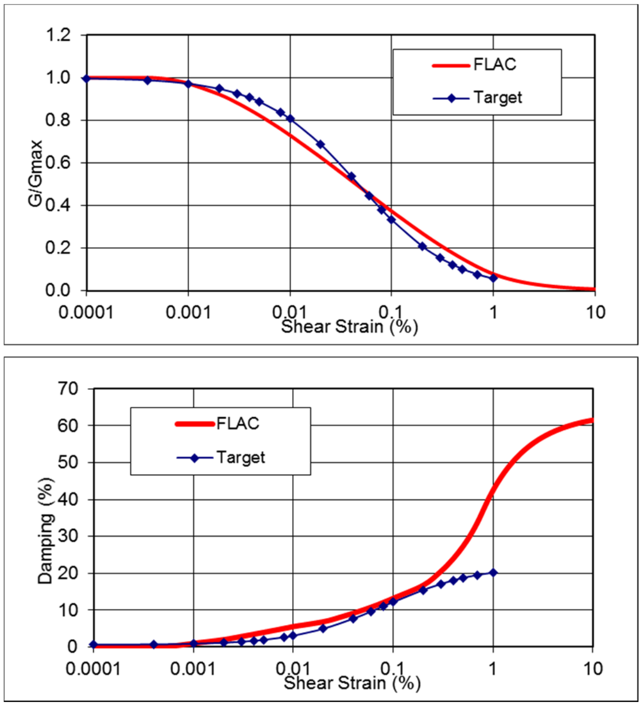

Figure 10. Matching of modulus reduction and damping curves used for clays and Darendeli experiments (2001).

The modulus reduction curves that we used in this study were based on Vucetic & Dobry (1991) for the clay materials (i.e., in the upper 30 m) and Darendeli (2001) for the sands (between 30 m and the base of our model at 45 m). Since FLAC uses mathematical expressions instead of curves, we matched the experimental curves by Vucetic and Dobry as well as Darendeli as close as possible in the main area of concern, i.e., for shear strains of 0.05% to 0.2% (as shown in Figures 9 and 10). Note that the damping shown in Figures 9 and 10 is directly obtained from the modulus reduction curves through the use of the Massing (1926) rule.

3.4 *Geogrid, rolling slab and panels*

The adopted MSE reinforcement in our analyses consisted of Tensar UX1400 geogrid, which is one of the weakest uniaxial geogrids in the UX series. This geogrid has a tensile strength of 27 kN/m at 5% strain. The geogrids were modeled in FLAC using axial elements (known in FLAC as cable elements).

Due to its thickness the concrete rolling slab, which seats on top of the LCC-MSE wall, was modeled using solid elements. To account for the inertial loads due to ballast, rails and similarly related machinery and equipment, the unit weight of these solid elements was increased appropriately.

The MSE wall's side panels were modeled in FLAC using liner beam elements having a thickness of 3 cm. These elements were given the properties of reinforced concrete and were directly attached to the end of the geogrid layers.

Figure 11 depicts the computed vertical stresses and tensile forces in the geogrid layer at the end of construction. Please note that the predicted tensile forces in the geogrid layers are less than 2% of its tensile strength. These tensile values are low due to the relatively high shear strength of the LCC materials.

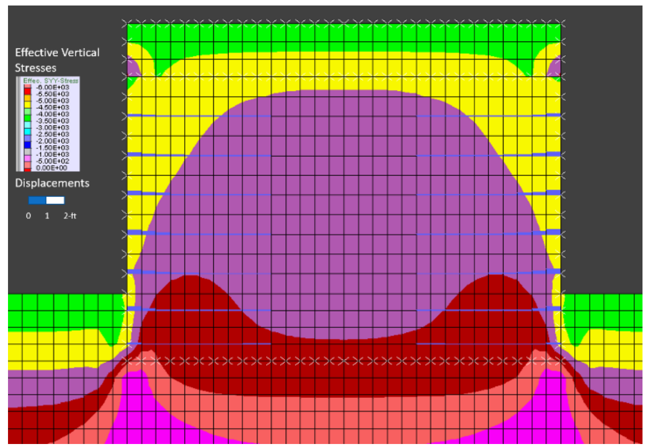

Figure 11. Computed geogrid tensile forces and vertical stresses in ground, LCC wall, and rolling slab.

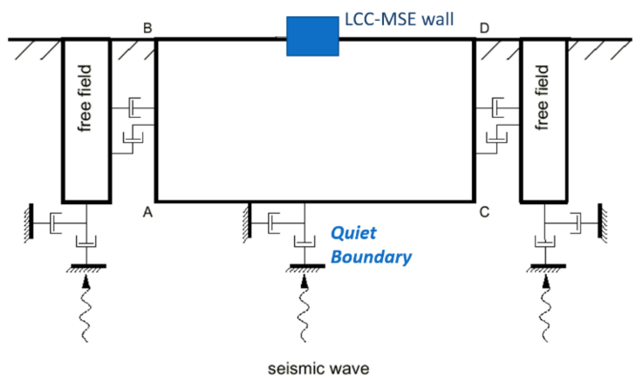

Figure 12. Quiet and free field boundaries used in FLAC.

4 GROUND MOTIONS AND NUMERICAL ANALYSES

To minimize wave reflections at model boundaries a quiet (viscous) boundary was specified along the base of the model, and free-field boundaries were specified along the edges, as shown in Figure 12.

The ground motions used in our analyses were obtained from existing records of earthquakes with magnitudes and accelerations similar to those anticipated at the San Jose site (Abrahamson, 2012) and included both Fault Parallel and Fault Normal components for each of the records.

The motions were spectrally matched (to the design spectral accelerations shown in Figure 13) using the software codes RspMatch and RspMatchEDT, pre and post processors for RspMatch (Abrahamson, 1992, and Geomotion, 2011a). The surface ground accelerations and spectral accelerations (before and after spectral matching) are shown in Figure 13.

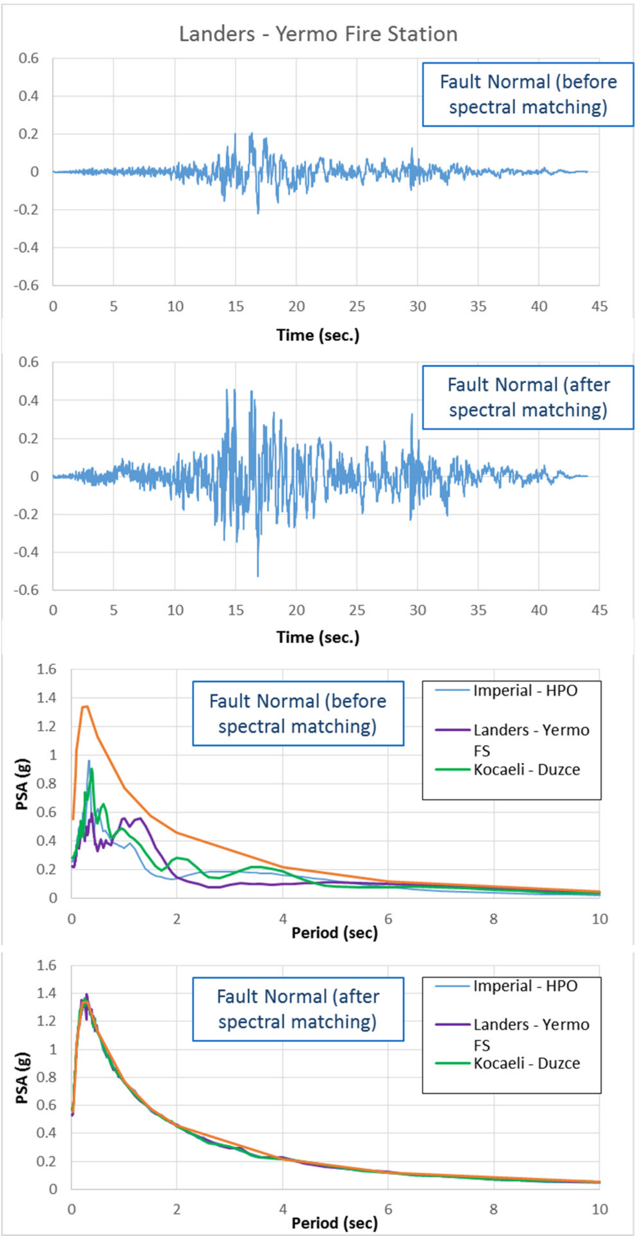

Figure 13. Accelerations (in g) of the 1992 Landers earthquake and spectral accelerations, before and after spectral matching.

Surface ground motions were deconvoluted in order to obtain the input velocities at the base of our FLAC model using the program SHAKE2000 (Geomotions, 2011b).

The results of our numerical simulations are shown in Figures 14 and 15. During our simulations, the computed maximum horizontal displacements ranged from 1 to 4 cm, and we predicted differential vertical movements from ¼ to 1½ cm.

Figures 14 and 15 show the deformed mesh in an exaggerated scale from the beginning (top plot) to the end of the earthquake (bottom plot). As can be seen the mesh moves mainly in a horizontal and quasi-rigid manner. Rocking of the LCC-MSE wall is very minor and not noticeable in Figures 14 and 15.

Because the reinforced concrete rolling slab at the top of the wall is heavy, it does create inertial overturning moments. However, these moments appear to be easily countered by the large base of the LCC-MSE wall which distributes them relatively evenly and prevents large vertical strains in the subgrade soils near the edges of the MSE wall.

Even during the most intense portion of the earthquake (mid-plots in Figures 14 and 15), the vertical and horizontal stresses are relatively evenly distributed throughout the base of the wall, and do not lead to a shearing along the base or bearing failures below the LCC-MSE wall. In summary, our model does not predict a soft ground failure of any type (shear, bearing, etc.). Similarly, our numerical analyses did not predict failure in the wall's LCC materials either, i.e., we did not observe tensile, shear or compressive failures of the LCC infill.

As seen in Figures 14 and 15, the side panels have inertial loads that pull on the geogrid layers and result in an increase of geogrid tensile forces. Figures 14 and 15 show that these tensile loads are almost immediately transferred to the LCC during an earthquake, and it appears that after approximately 2 m the geogrid has virtually no beneficial seismic role. Hence, the main role of geogrids appears to be for crack control purposes (e.g., cracks resulting from material shrinkage or minor differential movements resulting from varying bearing conditions).

5 CONCLUSIONS

Our numerical simulations were performed on a significantly weaker version of the LCC-MSE wall shown under construction in Figure 3, that was built at a soft clay site in the City of San Jose, for the Silicon Valley Rapid Transit system near San Francisco, California. The designers (GDC, 2014) used LCC for this wall in order to significantly lighten the load of an originally proposed traditional MSE wall which used soil as infill. The switch from soil to LCC was very successful and allowed the designers to completely eliminate the need for soil improvement under this MSE wall.

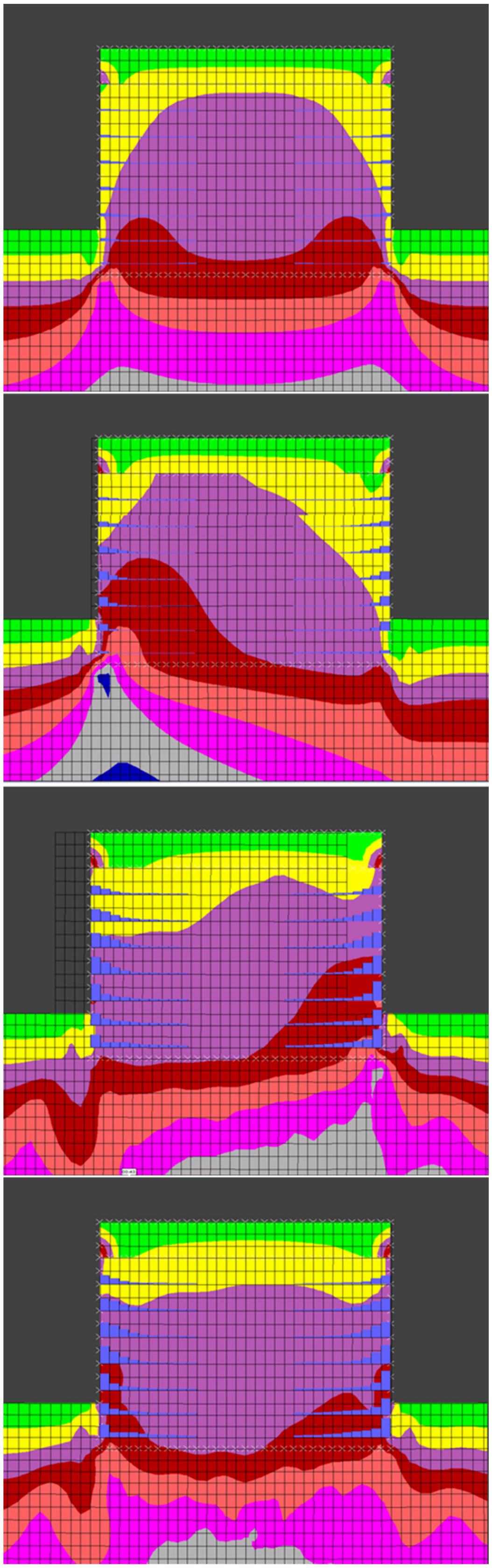

Figure 14. Deformed mesh, vertical stress contours and geogrid tensile loads (from beginning to end of earthquake).

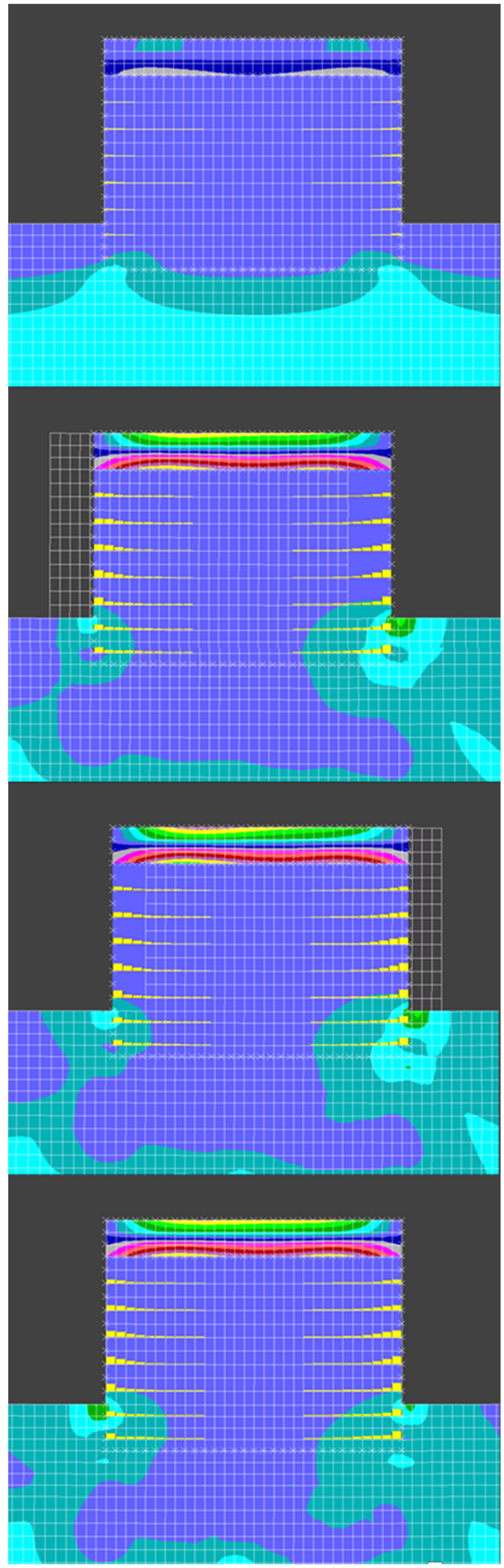

Figure 15. Deformed mesh, horizontal stress contours and geogrid tensile loads (from beginning to end of earthquake).

Our FLAC analyses indicate that on soft clay sites, LCC-MSE walls, such as the one analyzed herein, move in a quasi-rigid manner during earthquakes, i.e., they move mainly parallel to the ground surface and do not develop significant total or differential permanent vertical seismic movements.

Our numerical modeling which was conducted on a weaken version of a constructed LCC-MSE wall, did not predict ground failures (shear, bearing, sliding, overturning, etc.) under static (during construction) or under design seismic conditions. Similarly, failure of the LCC materials in either compressive, tensile or shear modes of failure was not predicted.

Our analyses indicate that the role of the geogrid reinforcement during earthquake loading is mainly to hold the side panels and that for seismic loading geogrid reinforcements provide little benefit to the wall beyond a distance of about 2 m from the face of the wall.

Hence, the main role of geogrids in LCC walls appears to be for crack control purposes (e.g., cracks resulting from material shrinkage and/or minor differential movements resulting from varying bearing conditions), and designers may consider limiting both the reinforcement lengths and type.

REFERENCES

Abrahamson, N.A. (1992). "*Non-stationary spectral matching*", Seismological Research Letters 63(1), 30.

Abrahamson, N. (2012) "Updated Peer Review of the 2005 ARS Curves for the Silicon Valley Rapid Transit Project," dated August 13, 2012.

ACI (2006). "*Guide for Cast-in-Place Low Density Cellular Concrete*", ACI-523.1 R-06.

Cell-Crete (2015), "Cellular Concrete Engineered Fill from Cell-Crete", www.cell-crete.com.

Chiu P., Pradel D. Et al. (2008), "*Seismic Response Analyses for the Silicon Valley Rapid Transit Project*", ASCE GSP 181, Geotechnical Earthquake Engineering and Soil Dynamics IV, Sacramento, 1-10.

Darendeli (2001). "*Development of a new family of normalized modulus reduction and material damping curves*", Ph.D. Dissertation, Dept. of Civil Engineering, Univ. of Texas, Austin, TX.

GDC (2014), "*Dynamic Numerical Analyses using FLAC for Lightweight Cellular Concrete MSE Walls for BART Berryessa Extension, San Jose, CA*", report by Group Delta Consultants dated July 11, 2014.

Geomotions (2011a), "*RspMatchEDT user manual",* www.geomotions.com/Download/RspMatchEDTManual.pdf.

Geomotions (2011b), "*SHAKE2000, user manual.*", www.geomotions.com/Download/SHAKE2000Manual.pdf.

Itasca (2011), "*FLAC (Fast Lagrangian Analysis of Continua) Version 7.0*", Minneapolis, USA, www.itascacg.com.

Masing, G. (1926), "*Eigenspannungen and verfertigung beim messing*", Proc. 2nd Int. Congress on Applied Mechanics, Zurich.

Teig J. and Anderson J. (2012). "*Innovative Design for the Colton Flyover Grade Separation of IPRR and BNSF, Colton, CA*" AREMA Annual Conference & Exposition.

Tiwari B. (2015a), "*Preliminary Result – Static Shear Strength of Lightweight Cellular Concrete Sample Batch 1*", report dated January 26.

Tiwari B. (2015b), "*G over Gmax & damping tests*", personal communication of April 4th.

Vucetic & Dobry (1991), "*Effect of Soil Plasticity on Cyclic Response", ASCE Journal of Geotechnical Engineering 117(1), 89-107.*